

Thermodynamics of Li^+ –Crown Ether Interactions in Aqueous Solvent

Ramón González-Pérez,[†] Stephen Adams,[†] Alexander W. Dowling,[†] William A.
Phillip,[†] and Jonathan K. Whitmer^{*,†}

[†]*Department of Chemical and Biomolecular Engineering, University of Notre Dame, Notre
Dame, Indiana 46556, USA*

[‡]*Department of Chemistry and Biochemistry, University of Notre Dame, Notre Dame,
Indiana 46556, USA*

E-mail: jwhitme1@nd.edu

Abstract

Lithium ion-based batteries are ubiquitous in modern technology due to applications in personal electronics and high-capacity storage for electric vehicles. Concerns about lithium supply and battery waste have prompted interest in lithium recycling methods. The crown ether, 12-crown-4, has been studied for its abilities to form stable complexes with lithium ions (Li^+). In this paper, molecular dynamics simulations are applied to examine the binding properties of a 12-crown-4 Li^+ system in aqueous solution. It was found that 12-crown-4 did not form stable complexes with Li^+ in aqueous solution due to the binding geometry which was prone to interference by surrounding water molecules. In addition, the binding properties of sodium ions (Na^+) to 12-crown-4 are examined for comparison. Subsequently, calculations were performed with the crown ethers 15-crown-5 and 18-crown-6 to study their complexation with Li^+ as well. It was determined that binding was unfavorable for both types of ions for all three crown ethers tested, though 15-crown-5 and 18-crown-6 showed a marginally greater affinity for Li^+ than 12-crown-4. Metastable minima present in the potential of mean force for Na^+ render binding marginally more likely there. We discuss these results in the context of membrane based applications of crown ethers for Li^+ separations.

Introduction

The transition to clean, renewable energy is a necessary task to both mitigate climate change and secure future energy production. Global treaties, such as the Paris Agreement, represent the commitment of a conglomerate of nations to work toward this end.¹ Efforts to reduce fossil fuel use and carbon outputs have led to increased interest in the use of Li^+ , particularly in the context of lithium-ion batteries (LIBs) as clean, renewable energy storage systems.²

Historically, lithium has been obtained from continental brines in the Salar de Atacama in Chile, the Andes Mountains in Argentina and other brine operations in Australia, whose lithium mining accounts for 54% of the world lithium production.^{3,4} Future

increase in lithium usage carries concerns about environmental effects and the stability of the lithium supply chain.⁵ Multiple potential sources should be explored, including the aforementioned concentrated brines, along with less concentrated (but relatively lithium-rich) seawater sources, and recycling of LIBs in electronic waste. Once spent, LIBs must be either discarded or recycled;⁶ disposal of LIBs carries environmental risks as LIBs may contain toxic elements such as mercury, lead, cadmium, copper, and zinc whose introduction to solid waste streams will have harmful effects on the environment.⁷ Disposal of this waste carries an opportunity cost as many of the minerals therein—lithium, copper,⁸ nickel,⁹ and cobalt¹⁰—are of high value for technology applications. It is therefore of interest to develop technologies that can extract lithium selectively from other molecules and ions present in each of these traditional and emerging sources.¹¹ Macrocyclic chemistry represents a promising method to enhance separation techniques (both membrane-based and adsorption-based) aimed at recovering or removing target metals^{12–15} from solution. Materials functionalized with strong-binding structures are of obvious utility in adsorption processes, but favorable binding in membrane separation processes can also induce mobility effects through the on-off kinetics associated with solute–ligand interactions. For instance, surface functionalized using favorable binding chemistries can be used to separate Li^+ ion from brines by slowing their overall dynamics through the membrane using host-guest interactions.¹⁶

The use of crown ethers as host molecules in functionalized membranes is one proposed method to recover lithium. Crown ethers are a heterocyclic molecule containing ether groups and are named according to the formula X-crown-Y, where X is the number of atoms in the ring and Y is the number of oxygen atoms.¹⁷ Since their discovery, crown ethers have been noted for their ability to form complexes with cations due to the electronegative cavity at their center of mass (COM).¹⁸ Due to the variance in sizes between different cations and different crown ether cavities, specific ions are hypothesized to have a greater affinity to certain crown ethers.¹⁹ Cavity sizes of 12-crown-4, 15-crown-5 and 18-crown-6 are 3.228, 4.074 and 5.299, where the lengths correspond to the minimum distance between two oxygen

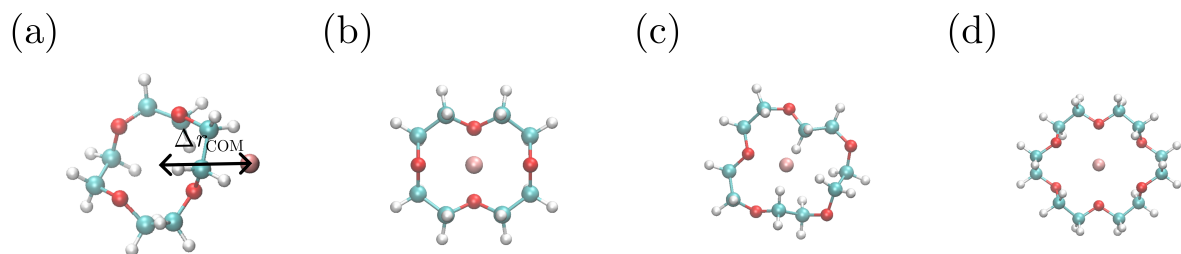


Figure 1: (a) Snapshot depicting the distance between Li^+ and the center of mass of a crown ether (12-crown-4), Δr_{COM} . Panels (b) to (d) depict snapshots of Li^+ at the center of mass of (b) 12-crown-4, (c) 15-crown-5 and (d) 18-crown-6. The color scheme for crown ethers and Li^+ is as follows: oxygen is red, carbon is cyan, lithium is ochre and hydrogen is white. See the methods section for a description of these parameters.

atoms located at para-position.²⁰ We illustrate hypothetical binding of a Li^+ ion to these three crown ethers in Figure 1.

It has been hypothesized, due to the relative size of metal cation species, that selective ion binding will result for the cation which best matches the size of the electronegative cavity; in a separations context, this effect should alter ion binding and effective transport, potentially enabling lithium recovery. Because the cavity size of crown ether 12-crown-4 corresponds to the size of the Li^+ , 12-crown-4 has garnered interest as a potential host for Li^+ .²¹ This work was supported by an initial set of density functional theory calculations that lend significant credence to the idea,²⁰ as do observations of improved alkali-metal ion separations when including CEs in non-aqueous environments.^{22–25} However, some other studies reveal that such size-matching predictions are not always realized.^{26,27} As the prevailing theory behind this work is done in vacuum, and experiments are typically done in a solvent, there is potential for discrepancies that can be resolved by appealing to molecular simulations.

A key quantity for determining the efficacy of separations involving host–guest binding (both adsorption and membrane-based separations) involves the partitioning of solute from the feed solution to the functionalized material (adsorbing surface or membrane). This partition is linked by fundamental thermodynamics to the binding affinity of a solute molecule to the host material. For example, in the context of adsorption processes, Eugene et al.²⁸

proposed a multiscale materials-process targeting framework that links molecular, device, and system design decisions to set material property targets that can be used to rapidly screen candidate sorbents. The molecular properties enter this multiscale model through the Langmuir isotherm, which relates the equilibrium loading q of solute on the sorbent to the concentration of solute in the effluent solution C by

$$q = \frac{K_d Q C}{1 + K_d C} . \quad (1)$$

This isotherm is described by two parameters the equilibrium binding constant, K_d , and saturation capacity, Q . The dissociation constant K_d is related to the standard binding free energy $\Delta G_{\text{bind}}^\circ$ by²⁹

$$\Delta G_{\text{bind}}^\circ = -k_B T \log (K_d C^\circ) . \quad (2)$$

where C° is the standard concentration of 1 M. In most studies, either the value of K_d or the value of $\Delta G_{\text{bind}}^\circ$ is reported, and these quantities are prominent in the design of new adsorptive materials.

Studies on Li^+ binding to crown ethers in water have been relatively scarce, with only a handful of existing experimental studies. One study³⁰ determined $\Delta G_{\text{bind}}^\circ = 0.5522 \text{ kJ mol}^{-1}$ of Li^+ (from LiCl) to 12-crown-4 using dipole-dipole relaxation time measurements in DHO (semiheavy water) solutions at 303.15 K, indicating that binding is unfavorable. Another study focused on the use of electromotive force measurements to determine the K_d of crown ether complexes.³¹ The measurements showed no formation of the 12-crown-4/ Li^+ complex and no $\Delta G_{\text{bind}}^\circ$ value is reported. In the literature, this is typically reported as $\Delta G_{\text{bind}}^\circ = 0$, though this is inconsistent with the definition of binding free energy from statistical mechanics,³² where $\Delta G_{\text{bind}}^\circ = 0$ would indicate roughly equal preference for the bound and unbound states at 1 M concentration. Additionally, some limited studies exist exploring the binding of Li^+ to 15-crown-5 and 18-crown-6. Nuclear magnetic resonance techniques have

been applied in which the chemical shift was used to determine the fraction of crown ethers bound and unbound to cations in various solvents.³³ The addition of Li^+ in water, however, did not significantly change the chemical shift, indicating a weak interaction between the crown ether and Li^+ ion. As a result, the $\log K_d$ values were reported as ~ 0 for 12-crown-4, 15-crown-5, and 18-crown-6. Ion-transfer polarography, a method in which the current is measured as the voltage is varied, determined the K_d of Li^+ and 18-crown-6 to be unity, again corresponding to a $\log(K_d)$ value of zero.³⁴ A study using calorimetric titrations, however, indicated favorable binding for Li^+ to 18-crown-6 and reported the value of $\log K_d$ to be greater than one.³⁵ In more recent, collaborative work between molecular simulation and experiment studying Li^+ transport through functionalized polymer membranes, stronger evidence was seen for Na^+ binding to crown ethers relative to Li^+ , and moreover, when Li^+ did bind, it was observed to be multiply coordinated by crown ethers.³⁶⁻³⁹ There are also other studies in which Li^+ binding is reported in methanol.⁴⁰

In this work, we use atomistic molecular simulations of crown ethers and ions in water to explore this binding affinity explicitly and understand the reasons behind the wide discrepancy between intuitive understanding of selective binding to crown ethers and observed binding affinity values. We focus on calculations of $\Delta G_{\text{bind}}^\circ$, and compute the binding energies of 12-crown-4, 15-crown-5 and 18-crown-6 to both Li^+ and Na^+ using Molecular Dynamics (MD) simulations and umbrella sampling to provide more theoretical information for the decision-making process of designing functionalized materials for lithium recovery. Importantly, rather than simply report on binding between crown ethers and Li^+ , we also explore binding of Na^+ , an ion which commonly occurs in brines alongside Li^+ and serves to provide a point of comparison for the efficacy of Li^+ binding. To determine error bars on the binding energies, the decorrelation time was estimated by averaging positional autocorrelation functions over the ensemble of umbrellas. Upon completion of the umbrella sampling runs, the free energy profile was generated using the weighted histogram analysis method (WHAM) using Grossfield’s implementation.⁵⁸

Methods

Structure files for the crown ether molecules were downloaded from the Automated Topology Builder (ATB) repository.^{59–61} Each crown ether molecule was then parameterized using Antechamber, a package in the AmberTools21 software suite.⁶² Initial configurations for the simulations were generated by constructing $(8\text{ nm})^3$ MD simulation boxes comprising one crown ether molecule, one Li^+ ion placed in the COM of the crown ether, one Cl^- ion placed in the vicinity of a corner of the box, and enough water molecules to give each species a concentration of 3.2 mM making sure the water density is within 1% its experimental value. Then, the total energy of the initial system was minimized using the steepest descent algorithm before subsequent equilibration and production runs. The general AMBER Force Field (GAFF) parameters,^{63,64} were used for describing bonded and nonbonded interactions in crown ethers, with TIP3P used for water, and the appropriate Joung–Cheatham parameters⁶⁵ for the nonbonding interactions of ions.

All simulations were performed using GROMACS 2018.3.^{66–73} The long-range electrostatic interactions were employed through a fast smooth Particle-Mesh Ewald technique with a ratio of the box dimensions and the spacing of 0.16 nm and an interpolation order of 4. The short-range cutoff distances of van der Waals and Coulombic interactions were both set to 1.2 nm. The bonds involving hydrogen atoms were constrained using the Parallel LINear Constraint Solver (P-LINCS) algorithm⁷⁴ with 4 as the highest order in the expansion of the constraint coupling matrix and 1 iteration to correct for rotational lengthening. For all MD simulations, the leap-frog algorithm was used to integrate Newtons equations of motion. Simulations were performed in the canonical (NVT) ensemble using a Bussi–Donadio–Parrinello thermostat⁷⁵ at 300 K. During the simulations, the coupling constants for the thermostat was set to 0.1 ps. Periodic boundary conditions were applied.

In molecular simulations, the time scale needed to visit more than one metastable state (e.g., one in which a guest particle is bound to a host molecule) is often longer than the ones used for simple MD. To improve sampling of those states the umbrella sampling technique

is used by adding a bias potential to the Hamiltonian of the system so that a collective variable corresponding to any structural parameter that could be measured throughout a simulation is held at selected target values. An added benefit of umbrella sampling is the ability to reconstruct a Potential of Mean Force (PMF, here equivalent to the free energy $F(\Delta r_{\text{COM}})$ measured along a reaction coordinate Δr_{COM}). To initialize configurations for umbrella sampling, a 1 fs timestep MD simulation was run at equilibrium for 40, 20 and 60 ns for the 12-crown-4, 15-crown-5 and 18-crown-6, respectively. The different simulation times were chosen in order to ensure the system reached configurations with different crown ether COM–Li⁺ distances between 0 and 4 nm to perform umbrella sampling runs. These configurations were distributed on the Δr_{COM} domain in two groups: one set is evenly spaced on the interval from 0.0 to 4.0 nm with a spacing of 0.2 nm (twenty-one independent configurations) to cover the entire simulation box and a second set focused on the “binding” domain from 0.0 to 0.5 nm with a spacing of 0.025 nm (eighteen additional configurations since 0.0, 0.2 and 0.4 nm are already part of the first group) to ensure features in this region are accurately captured. Each individual configuration was then again equilibrated for 1 ns with a timestep of 1 fs before recording statistics for umbrella sampling. Free energy calculations with umbrella sampling were used to determine the PMF of the systems. The reaction coordinate selected for the PMF was the center-of-mass distance between the crown ethers and Li⁺. K_{d} can be determined from the PMF by computing the ratio of partition integrals over the bound and unbound states:⁷⁶

$$K_{\text{d}}C^{\circ} = \frac{\int_{\text{bound}} \exp\left(\frac{-F(\xi)}{RT}\right) d\xi}{\int_{\text{unbound}} \exp\left(\frac{-F(\xi)}{RT}\right) d\xi} \quad (3)$$

where $\xi = \Delta r_{\text{COM}}$. For the purposes of numerical integration, we shift $F(\xi)$ such that $F(\xi) := 0$ at its lowest point when the ion is bound, provided there is a well-defined bound state. Note that the unbound state is defined to be volume-corrected to 1 M concentration.⁷⁷

Each umbrella production run was performed for 400 ns with a timestep of 2 fs. The umbrella bias used a spring constant of 62.3584 kJ mol⁻¹nm⁻², chosen to balance confinement

with overlap between neighboring umbrellas. Umbrella sampling was implemented using the open-source, community-developed PLUMED library,⁷⁸ version 2.5.0.⁷⁹ Upon completion of the umbrella sampling runs, for each run, correlation time was determined by estimating the autocorrelation function of the collective variable over time and then fitted to an exponential function. The decorrelation time was used to subsample the datasets for Monte Carlo bootstrap error analysis. Then, the free energy profiles were generated using Grossfield’s implementation of the WHAM method.⁵⁸

Results and Discussion

To ensure that sufficient decorrelated statistics are gathered in our simulation runs, we compute a set of time-correlation functions of the distance between Li^+ and the various crown ethers, defined by the relation

$$\Xi_i(t) := \frac{\langle \xi(t)\xi(0) \rangle_i}{\langle \xi(0)^2 \rangle_i} \quad (4)$$

where the subscript i denotes averaging over the trajectory within umbrella i . These are plotted for Li^+ systems in Figure 2. These suggest that most systems exhibit rather swift decorrelation on the scale of the simulation. We can reduce this to a single representative timescale using the averaged form $\bar{\Xi}(t) = \frac{1}{N} \sum_{i=1}^N \Xi_i(t)$ which suggests systems are typically decorrelated by a time $\tau = 2000$ ps. The value of τ is subsequently used in the WHAM algorithm.

The PMFs calculated are expressed as a Helmholtz free energy, $\Delta F(\Delta r_{CM})$, and are plotted in Figure 3. Note that this differs slightly from the Gibbs energy that is the natural measurement in constant-temperature, constant-pressure experiments, as the Helmholtz free energy is measured in systems in which the volume and temperature are held constant. When the product of pressure and volume is essentially constant over the domain of the CV, $\Delta G(\Delta r_{CM})$ will be approximately the same as the ΔF we calculate here.⁷⁷ Thus for systems

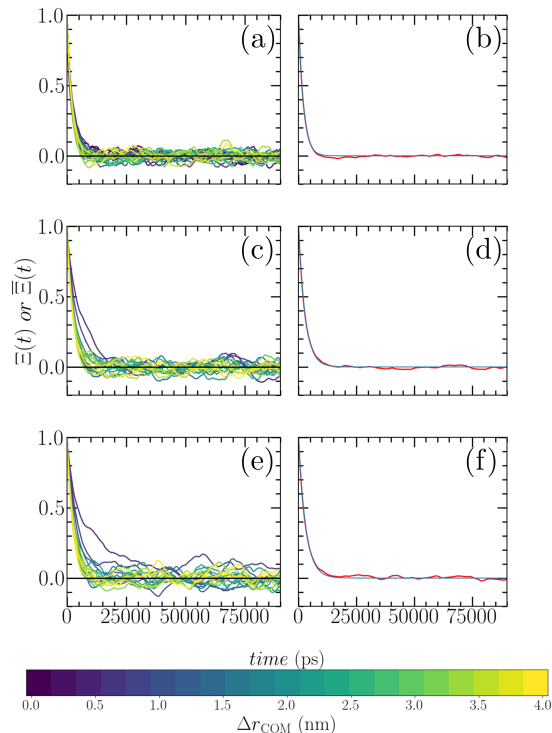


Figure 2: Time-correlation functions, $\Xi(t)$, of the distance between Li^+ and (a) 12-crown-4, (c) 15-crown-5 and (e) 18-crown-6 for different Δr_{COM} values. Panels (b), (d) and (f) correspond to the average of the time-correlation functions, $\bar{\Xi}(t)$, in (a), (c) and (e), respectively.

in which pressure and volume changes are can be justified as sufficiently small on average over the course of a simulation, as was verified for these systems, the differences between ΔG and ΔF are negligible.

Referring to our calculated PMFs, a striking feature is immediately evident in each of the calculations of crown-ether- Li^+ binding which contradicts with many accounts in the published literature (cf. Table 1 and Ref.²⁸)—while metastable states exist in the small Δr_{COM} region, there is not a stable binding basin to compete with the entropy of the separated state. Put simply, these PMFs predict that under reasonably dilute conditions, Li^+ will not bind to to crown ethers. This is not to state that some marginally favorable conditions do not exist; favorable energetic interactions between the Li^+ ion and oxygens in the crown ether lead to a collection of metastable states. Indeed, the Li^+ ion demonstrates three metastable states between Δr_{COM} of 0.0 and 1.0 nm with 12-crown-4.

Similarly, the interactions with both 15-crown-5 and 18-crown-6 exhibit reasonably deep metastable minima, with 18-crown-6 giving the deepest binding energies. While Li^+ exhibits a binding mode to 12-crown-4, selectivity with respect to other ions must be considered. The PMF calculations performed with Na^+ are shown in Figures 3 (d-f). By contrast, Na^+ exhibits what appears to be marginally better binding affinity, particularly for 12-crown-4 and 15-crown-5; a deep metastable minimum appears for Na^+ -12-crown-4 interactions (Fig. 3(d)), while a global minimum with limited entropy appears in the PMF for Na^+ -15-crown-5 interactions (Fig. 3(e)). Association constants and binding energies published in the literature for Na^+ -crown ether complexes are shown in Table 2. When integrated over the regions close to zero (effectively the “bound” regime) and the entropically dominated (“unbound”) regime none of the alkali metal ion-crown ether systems analysed exhibits favorable binding at standard 1 M concentration. The standardized $\Delta G_{\text{bind}}^\circ$ values resulting from our PMF calculations are shown in Table 3. From this we must conclude that no binding between crown ethers and Li^+ in aqueous solution is indicated by these simulations.

Note that there are a few potential criticisms to these conclusions that we should address. The first is that we have explored only one force field (GAFF⁶³); it is possible that others are better at representing the interaction between crown ethers and alkali ions. We note that recent simulations examining crown-ether inclusions in separation membranes using the OPLS force field found unexpectedly poor binding for Li^+ -crown-ether complexes.³⁶⁻³⁹ The typical simulations were performed in a more concentrated environment where multiple crown ether molecules could complex to a Li^+ ion, and some binding was observed, but was weaker than anticipated based on the prevailing literature. This supports the hypothesis that, at least among classical fixed-charge, non-polarizable models, this result will generalize. A second potential criticism is that proper resolution of the hard Li^+ binding to crown ether is likely to influence the local electronic environment significantly, and a polarizable model (classical drude,^{80,81} AMOEBA,^{82,83} or ab-initio MD⁸⁴) is necessary to resolve this effect. This is a distinct possibility, but one which must be considered, as no calculations

have to-date considered the effects of polarization on Li^+ -crown ether binding in aqueous solution. However, given the prior results compiled in Table 1, the anticipated effects are likely to be minimal — no significant binding to isolated crown ethers has been observed experimentally. Though some studies using functionalized nanoparticles or brushes with crown-ether moieties have seen modest binding,²⁸ their interpretation has been predicated on a 1:1 binding mechanism which the fundamental studies (including this one) do not support in an aqueous environment. Finally, the point may be raised that applications of crown ethers (e.g.) in adsorption or membrane separation processes will need to examine binding within an effectively more concentrated environment. This can have the effect of turning the metastable minima observed in Fig. 3 into stable minima by increasing their depth via multiple coordination and limiting entropic competition. It must be kept in mind there that lithium still exists in relatively dilute concentration, meaning the $\log K_d$ may shift toward slightly more favorable values due to these effects (see, e.g., Ref.³⁸), but that does not make binding a favorable outcome on the scale necessary for engineering applications.²⁸ Moreover, the primary competitor of Li^+ in many aqueous sources (Na^+) is orders of magnitude more abundant³⁶ while concomitantly exhibiting more favorable binding according to our PMFs. Essentially, we anticipate that CEs are non-functional for adsorption separations, while any effects observed on the relative mobility of Li^+ and other ions in the solution are likely insufficient for performing meaningful separations in the aqueous phase.

Conclusion

Motivated by their potential use in lithium resource recovery, we have in this work performed atomistic simulations investigating the binding between alkali metal ions and crown ethers in aqueous solvent. Surprisingly, we found no evidence for favorable formation of Li^+ -crown-ether complexes, and only weak association in Na^+ -crown-ether complexes. While these calculations are limited by the choice of a fixed-charge, all-atom model, taken alongside

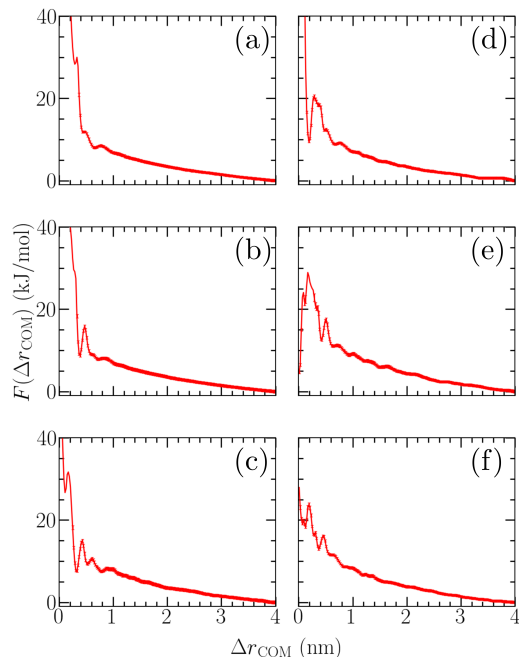


Figure 3: PMFs of the distance between Li^+ and (a) 12-crown-4, (b) 15-crown-5 and (c) 18-crown-6 and Na^+ and (d) 12-crown-4, (e) 15-crown-5 and (f) 18-crown-6 for different Δr_{COM} values.

mixed-to-negative findings regarding binding in the experimental literature, we anticipate a more detailed model will change the results quantitatively, but not qualitatively. The message from this work is clear; crown ether-based technologies for chelation of Li^+ are not feasible based on 1:1 binding assumptions. Indeed, it is observed that neither Li^+ nor Na^+ bind well to crown-ethers, with deeper metastable minima occurring for Na^+ . It remains possible that crown-ether-like environments can take advantage of favorable enthalpic association between Li^+ and ether oxygens through multivalent binding or local solvation preferable to water—such multiple-association is supported by simulations.^{36–39} This presents a compelling hypothesis to be tested in future research.

Acknowledgments

RGP, SA, and JKW are grateful to support from the Department of Energy, Basic Energy Sciences, Materials Science and Engineering Division, through the Midwest Integrated Cen-

ter for Computational Materials (MICCoM) for funding the exploration and application of advanced sampling algorithms used in this work. AWD and WAP acknowledge support from the United States National Science Foundation through award CBET-2147605.

References

- (1) Agreement, P. Paris agreement. Report of the Conference of the Parties to the United Nations Framework Convention on Climate Change (21st Session, 2015: Paris). 2015; p 2017.
- (2) Manthiram, A. An Outlook on Lithium Ion Battery Technology. *ACS Central Science* **2017**, *3*, 1063–1069.
- (3) Kelly, J. C.; Wang, M.; Dai, Q.; Winjobi, O. Energy, greenhouse gas, and water life cycle analysis of lithium carbonate and lithium hydroxide monohydrate from brine and ore resources and their use in lithium ion battery cathodes and lithium ion batteries. *Resources, Conservation and Recycling* **2021**, *174*, 105762.
- (4) US Geological Survey, 2020. Mineral Commodity Summaries, 2020.
- (5) Lithium-ion Battery Sector: Developing a Promising Sector for Quebecs Economy. 2019.
- (6) Shekhar, A. R.; Parekh, M. H.; Pol, V. G. Worldwide ubiquitous utilization of lithium-ion batteries: What we have done, are doing, and could do safely once they are dead? *Journal of Power Sources* **2022**, *523*, 231015.
- (7) Tabelin, C. B.; Dallas, J.; Casanova, S.; Pelech, T.; Bournival, G.; Saydam, S.; Canbulat, I. Towards a low-carbon society: A review of lithium resource availability, challenges and innovations in mining, extraction and recycling, and future perspectives. *Minerals Engineering* **2021**, *163*, 106743.

- (8) Ferreira, D. A.; Prados, L. M. Z.; Majuste, D.; Mansur, M. B. Hydrometallurgical separation of aluminium, cobalt, copper and lithium from spent Li-ion batteries. *Journal of Power Sources* **2009**, *187*, 238–246.
- (9) Lupi, C.; Pasquali, M.; Dell’Era, A. Nickel and cobalt recycling from lithium-ion batteries by electrochemical processes. *Waste Management* **2005**, *25*, 215–220.
- (10) Pagnanelli, F.; Moscardini, E.; Altimari, P.; Abo Atia, T.; Toro, L. Cobalt products from real waste fractions of end of life lithium ion batteries. *Waste Management* **2016**, *51*, 214–221.
- (11) Wamble, N. P.; Eugene, E. A.; Phillip, W. A.; Dowling, A. W. Optimal Diafiltration Membrane Cascades Enable Green Recycling of Spent Lithium-Ion Batteries. *ACS Sustainable Chemistry & Engineering* **2022**, *10*, 12207–12225.
- (12) Shin, S. M.; Kim, N. H.; Sohn, J. S.; Yang, D. H.; Kim, Y. H. Development of a metal recovery process from Li-ion battery wastes. *Hydrometallurgy* **2005**, *79*, 172–181.
- (13) Bi, H.; Zhu, H.; Zu, L.; Bai, Y.; Gao, S.; Gao, Y. A new model of trajectory in eddy current separation for recovering spent lithium iron phosphate batteries. *Waste Management* **2019**, *100*, 1–9.
- (14) Marinos, D.; Mishra, B. An Approach to Processing of Lithium-Ion Batteries for the Zero-Waste Recovery of Materials. *Journal of Sustainable Metallurgy* **2015**, *1*, 263–274.
- (15) Zhan, R.; Oldenburg, Z.; Pan, L. Recovery of active cathode materials from lithium-ion batteries using froth flotation. *Sustainable Materials and Technologies* **2018**, *17*, e00062.
- (16) Zhang, Y.; Wang, L.; Sun, W.; Hu, Y.; Tang, H. Membrane technologies for $\text{Li}^+/\text{Mg}^{2+}$ separation from salt-lake brines and seawater: A comprehensive review. *Journal of Industrial and Engineering Chemistry* **2020**, *81*, 7–23.

- (17) Stillwell, W. *An introduction to biological membranes: composition, structure and function*; Elsevier, 2016.
- (18) Klampff, C. W. In *Quantitation of amino acids and amines by chromatography*; Molnr-Perl, I., Ed.; Journal of Chromatography Library; Elsevier, 2005; Vol. 70; pp 525–558.
- (19) Goldshleger, N. F.; Chernyak, A. V.; Lobach, A. S.; Kalashnikova, I. P.; Baulin, V. E.; Tsivadze, A. Y. Monomerization of crown-containing phthalocyanines in microheterogeneous organized systems. *Protection of Metals and Physical Chemistry of Surfaces* **2015**, *51*, 212–220.
- (20) Yao, Y. L.; Zhu, M. Y.; Zhao, Z.; Liu, W. G.; Tong, B. H.; Li, M. Y. Density functional theory study of selectivity of crown ethers to Li^+ in spent lithium-ion batteries leaching solutions. *Chinese Journal of Chemical Physics* **2019**, *32*, 343–348.
- (21) Torrejos, R. E. C.; Nisola, G. M.; Song, H. S.; Limjuco, L. A.; Lawagon, C. P.; Parohinog, K. J.; Koo, S.; Han, J. W.; Chung, W. J. Design of lithium selective crown ethers: Synthesis, extraction and theoretical binding studies. *Chemical Engineering Journal* **2017**, *326*, 921–933.
- (22) Qi, Z.; Cussler, E. Membrane separation of potassium nitrate from mixed brines. *Journal of Membrane Science* **1984**, *19*, 259–272.
- (23) Reusch, C. F.; Cussler, E. L. Selective membrane transport. *AIChE Journal* **1973**, *19*, 736–741.
- (24) Oral, I.; Abetz, V. A Highly Selective Polymer Material using Benzo-9-Crown-3 for the Extraction of Lithium in Presence of Other Interfering Alkali Metal Ions. *Macromolecular Rapid Communications* **2021**, *42*, 2000746.
- (25) Caracciolo, F.; Cussler, E. L.; Evans, D. F. Membranes with common ion pumping. *AIChE Journal* **1975**, *21*, 160–167.

- (26) Anderson, J. D.; Paulsen, E. S.; Dearden, D. V. Alkali metal binding energies of dibenzo-18-crown-6: Experimental and computational results. *International Journal of Mass Spectrometry* **2003**, *227*, 63–76.
- (27) More, M. B.; Ray, D.; Armentrout, P. B. Intrinsic affinities of alkali cations for 15-crown-5 and 18-crown-6: Bond dissociation energies of gas-phase M^+ -crown ether complexes. *Journal of the American Chemical Society* **1999**, *121*, 417–423.
- (28) Eugene, E. A.; Phillip, W. A.; Dowling, A. W. Material Property Targets to Enable Adsorptive Water Treatment and Resource Recovery Systems. *ACS ES&T Engineering* **2021**, *1*, 1171–1182.
- (29) Gumbart, J. C.; Roux, B.; Chipot, C. Efficient determination of protein-protein standard binding free energies from first principles. *Journal of Chemical Theory and Computation* **2013**, *9*, 3789–3798.
- (30) Erk, Ç. Determination of the association constants of macrocyclic ethers by the aid of ^{13}C dipole-dipole relaxation time measurements. Part. I., Li^+ , Mg^{2+} and Ca^{2+} complexes of 1,4,7,10-tetraoxacyclododecane. *Spectroscopy Letters* **1985**, *18*, 723–730.
- (31) Høiland, H.; Ringseth, J. A.; Brun, T. S. Cation-Crown Ether Complex Formation in Water. II. Alkali and Alkaline Earth Cations and 12-Crown-4, 15-Crown-5, and 18-Crown-6. *Journal of Solution Chemistry* **1979**, *8*, 779–792.
- (32) Dill, K.; Bromberg, S. *Molecular Driving Forces: Statistical Thermodynamics in Biology, Chemistry, Physics, and Nanoscience*; Garland Science, 2010.
- (33) Smetana, A. J.; Popov, A. I. Lithium-7 nuclear magnetic resonance and calorimetric study of lithium crown complexes in various solvents. *Journal of Solution Chemistry* **1980**, *9*, 183–196.

- (34) Kudo, Y.; Takeda, Y.; Matsuda, H. On the facilitating effect of neutral macrocyclic ligands on ion transfer across the interface between aqueous and organic solutions II: Alkali metal ion complexes with hydrophilic crown ethers. *Journal of Electroanalytical Chemistry* **1995**, *396*, 333–338.
- (35) Buschmann, H. J.; Cleve, E.; Schollmeyer, E. Complex formation between alkali and alkaline earth cations and crown ethers and cryptands in aqueous solution. *Journal of Coordination Chemistry* **1996**, *39*, 293–298.
- (36) Zofchak, E.; Wheatle, B.; Zhang, Z.; Freeman, B.; Ganesan, V. Origins of Permselectivity in Lithium/Sodium Reverse-Selective 12-crown-4 Ether Functionalized Polymer Membranes. APS March Meeting Abstracts. 2021; pp B04–010.
- (37) Zofchak, E. S.; Zhang, Z.; Wheatle, B. K.; Sujanani, R.; Warnock, S. J.; Dilenschneider, T. J.; Hanson, K. G.; Zhao, S.; Mukherjee, S.; Abu-Omar, M. M. et al. Origins of Lithium/Sodium Reverse Permeability Selectivity in 12-Crown-4-Functionalized Polymer Membranes. *ACS Macro Letters* **2021**, *10*, 1167–1173.
- (38) Warnock, S. J.; Sujanani, R.; Zofchak, E. S.; Zhao, S.; Dilenschneider, T. J.; Hanson, K. G.; Mukherjee, S.; Ganesan, V.; Freeman, B. D.; Abu-Omar, M. M. et al. Engineering Li/Na selectivity in 12-Crown-4-functionalized polymer membranes. *Proceedings of the National Academy of Sciences of the United States of America* **2021**, *118*, 1–8.
- (39) Zofchak, E.; Zhang, Z.; Marioni, N.; Duncan, T.; Sachar, H.; Freeman, B.; Ganesan, V. Origins of cation-cation selectivity in crown ether-functionalized polymer membranes. *Bulletin of the American Physical Society* **2022**,
- (40) Inoue, Y.; Hakushi, T.; Liu, Y.; Tong, L. H. Molecular design of crown ethers. 12. Complexation thermodynamics of 12-to 16-crown-4: Thermodynamic origin of high

lithium selectivity of 14-crown-4. *The Journal of Organic Chemistry* **1993**, *58*, 5411–5413.

- (41) Dipole-dipole relaxation time measurement in DHO at 303.15 K.
- (42) ^{13}C NMR relaxation-time measurement in DHO at 298.15 K.
- (43) Erk, Ç. *NMR in Supramolecular Chemistry*; 1999; pp 315–318.
- (44) Electromotive force measurement.
- (45) Nuclear Magnetic Resonance at 300.15 K.
- (46) Ion transfer polarography.
- (47) Calculated from calorimetric titrations.
- (48) Density Functional Theory using the conductor like screening model (COSMO) in DMol³.
- (49) Study of Li selectivity in 12-crown-4–functionalized polymer membranes. NMR spectroscopy was used to determine binding constants for a norbornene-12-crown-4 monomer (1.98) and a representative polynorbornene homopolymer with pendant 12-crown-4 moieties on each repeat unit (1.77).
- (50) ^{13}C NMR relaxation-time measurement in DHO at 298.15 K.
- (51) Electromotive force measurement.
- (52) Electromotive force measurement.
- (53) Electromotive force measurement.
- (54) Calorimetric titration study at 298.15 K and $\mu = 0.1$.

- (55) Izatt, R.; Terry, R.; Haymore, B.; Hansen, L.; Dalley, N.; Avondet, A.; Christensen, J. Calorimetric titration study of the interaction of several uni- and bivalent cations with 15-crown-5, 18-crown-6, and two isomers of dicyclohexo-18-crown-6 in aqueous solution at 25 °C and $\mu = 0.1$. *Journal of the American Chemical Society* **1976**, *98*, 7620–7626.
- (56) Calorimetric titration study at 298.15 K and $\mu = 0.1$.
- (57) Calculated from calorimetric titrations.
- (58) Grossfield, A. An Implementation of WHAM: The Weighted Histogram Analysis Method, version 2.0.10.1. http://membrane.urmc.rochester.edu/wordpress/?page_id=126
- (59) Malde, A. K.; Zuo, L.; Breeze, M.; Stroet, M.; Poger, D.; Nair, P. C.; Oostenbrink, C.; Mark, A. E. An Automated force field Topology Builder (ATB) and repository: Version 1.0. *Journal of Chemical Theory and Computation* **2011**, *7*, 4026–4037.
- (60) Canzar, S.; El-Kebir, M.; Pool, R.; Elbassioni, K.; Mark, A. E.; Geerke, D. P.; Stougie, L.; Klau, G. W. Charge group partitioning in biomolecular simulation. *Journal of Computational Biology* **2013**, *20*, 188–198.
- (61) Koziara, K. B.; Stroet, M.; Malde, A. K.; Mark, A. E. Testing and validation of the Automated Topology Builder (ATB) version 2.0: Prediction of hydration free enthalpies. *Journal of Computer-Aided Molecular Design* **2014**, *28*, 221–233.
- (62) Wang, J.; Wang, W.; Kollman, P. A.; Case, D. A. Automatic atom type and bond type perception in molecular mechanical calculations. *Journal of Molecular Graphics and Modelling* **2006**, *25*, 247–260.
- (63) Wang, J.; Wolf, R. M.; Caldwell, J. W.; Kollman, P. A.; Case, D. A. Development and testing of a general Amber force field. *Journal of Computational Chemistry* **2004**, *25*, 1157–1174.

- (64) Case, A.; Aktulga, H.; Belfon, K.; Ben-Shalom, I.; Brozell, S.; Cerutti, D.; Cheatham III, T.; Cisneros, G.; Cruzeiro, V.; Darden, T. et al. Amber 2021, University of California, San Francisco. [(accessed on 1 February 2022)].
- (65) Joung, I. S.; Cheatham, T. E. Determination of alkali and halide monovalent ion parameters for use in explicitly solvated biomolecular simulations. *Journal of Physical Chemistry B* **2008**, *112*, 9020–9041.
- (66) Bekker, H.; Berendsen, H.; Dijkstra, E.; Achterop, S.; Vondrumen, R.; van der Spoel, D.; Sijbers, A.; Keegstra, H.; Renardus, M. GROMACS - A parallel computer for molecular-dynamics simulations. 4th International Conference on Computational Physics (PC 92). 1993; pp 252–256.
- (67) Berendsen, H. J.; van der Spoel, D.; van Drunen, R. GROMACS: A message-passing parallel molecular dynamics implementation. *Computer Physics Communications* **1995**, *91*, 43–56.
- (68) Lindahl, E.; Hess, B.; van der Spoel, D. GROMACS 3.0: A package for molecular simulation and trajectory analysis. *Journal of Molecular Modeling* **2001**, *7*, 306–317.
- (69) van der Spoel, D.; Lindahl, E.; Hess, B.; Groenhof, G.; Mark, A. E.; Berendsen, H. J. GROMACS: Fast, flexible, and free. *Journal of Computational Chemistry* **2005**, *26*, 1701–1718.
- (70) Hess, B.; Kutzner, C.; van der Spoel, D.; Lindahl, E. GRGMACS 4: Algorithms for highly efficient, load-balanced, and scalable molecular simulation. *Journal of Chemical Theory and Computation* **2008**, *4*, 435–447.
- (71) Pronk, S.; Páll, S.; Schulz, R.; Larsson, P.; Bjelkmar, P.; Apostolov, R.; Shirts, M. R.; Smith, J. C.; Kasson, P. M.; Van Der Spoel, D. et al. GROMACS 4.5: A high-throughput and highly parallel open source molecular simulation toolkit. *Bioinformatics* **2013**, *29*, 845–854.

- (72) Páll, S.; Abraham, M. J.; Kutzner, C.; Hess, B.; Lindahl, E. Tackling exascale software challenges in molecular dynamics simulations with GROMACS. International conference on exascale applications and software. 2014; pp 3–27.
- (73) Abraham, M. J.; Murtola, T.; Schulz, R.; Páll, S.; Smith, J. C.; Hess, B.; Lindahl, E. GROMACS: High performance molecular simulations through multi-level parallelism from laptops to supercomputers. *SoftwareX* **2015**, *1-2*, 19–25.
- (74) Hess, B. P-LINCS: A parallel linear constraint solver for molecular simulation. *Journal of Chemical Theory and Computation* **2008**, *4*, 116–122.
- (75) Bussi, G.; Donadio, D.; Parrinello, M. Canonical sampling through velocity rescaling. *Journal of Chemical Physics* **2007**, *126*, 014101.
- (76) Doudou, S.; Burton, N. A.; Henchman, R. H. Standard free energy of binding from a one-dimensional potential of mean force. *Journal of Chemical Theory and Computation* **2009**, *5*, 909–918.
- (77) Leonhard, A. C.; Whitmer, J. K. Accurate Determination of Cavitand Binding Free Energies via Unrestrained Advanced Sampling. *Journal of Chemical Theory and Computation* **2019**, *15*, 5761–5768.
- (78) Promoting transparency and reproducibility in enhanced molecular simulations. *Nature methods* **2019**, *16*, 670–673.
- (79) Tribello, G. A.; Bonomi, M.; Branduardi, D.; Camilloni, C.; Bussi, G. PLUMED 2: New feathers for an old bird. *Computer Physics Communications* **2014**, *185*, 604–613.
- (80) Li, H.; Chowdhary, J.; Huang, L.; He, X.; MacKerell, A. D.; Roux, B. Drude Polarizable Force Field for Molecular Dynamics Simulations of Saturated and Unsaturated Zwitterionic Lipids. *Journal of Chemical Theory and Computation* **2017**, *13*, 4535–4552.

- (81) Lemkul, J. A.; Roux, B.; Van Der Spoel, D.; Mackerell, A. D. Implementation of extended Lagrangian dynamics in GROMACS for polarizable simulations using the classical Drude oscillator model. *Journal of Computational Chemistry* **2015**, *36*, 1473–1479.
- (82) Ren, P.; Ponder, J. W. Consistent treatment of inter- and intramolecular polarization in molecular mechanics calculations. *Journal of Computational Chemistry* **2002**, *23*, 1497–1506.
- (83) Ren, P.; Ponder, J. W. Polarizable atomic multipole water model for molecular mechanics simulation. *The Journal of Physical Chemistry B* **2003**, *107*, 5933–5947.
- (84) Marx, D.; Hutter, J. *Ab initio molecular dynamics: basic theory and advanced methods*; Cambridge University Press, 2009.

Table 1: Association constants and binding energies found in the literature for Li^+ -crown ether complexes

Crown ether	K_d or $\Delta G_{\text{bind}}^\circ$	Reference
12-crown-4	$\Delta G_{\text{bind}}^\circ = 0.5522 \text{ kJ mol}^{-1}$ ⁴¹	30
12-crown-4	$\log K_d = -0.55$ ⁴²	43
12-crown-4	$K_d = 0$ (no binding) ⁴⁴	31
12-crown-4	$\log K_d \sim 0$ (no binding) ⁴⁵	33
15-crown-5	$\log K_d \sim 0$ (no binding)	33
18-crown-6	$\log K_d \sim 0$ (no binding)	33
18-crown-6	$\log K_d = 0$ (no binding) ⁴⁶	34
18-crown-6	$\log K_d > 1$ ⁴⁷	35
12-crown-4	$\Delta G_{\text{bind}}^\circ = -120.15 \text{ kJ mol}^{-1}$ ⁴⁸	20
15-crown-5	$\Delta G_{\text{bind}}^\circ = -141.36 \text{ kJ mol}^{-1}$	20
18-crown-6	$\Delta G_{\text{bind}}^\circ = -91.99 \text{ kJ mol}^{-1}$	20
12-crown-4	$\log K_d = 1.98, 1.77$ ⁴⁹	38

Table 2: Association constants and binding energies found in the literature for Na^+ -crown ether complexes

Crown ether	K_d or $\Delta G_{\text{bind}}^\circ$	Reference
18-crown-6	$\log K_d = 1.18$ ⁵⁰	43
12-crown-4	$K_d = 0$ (no binding) ⁵¹	31
15-crown-5	$K_d = 4.7 \pm 0.3$ ⁵²	31
18-crown-6	$K_d = 6.6 \pm 0.3$ ⁵³	31
15-crown-5	$K_d = 5.0 \pm 1$ ⁵⁴	55
18-crown-6	$K_d = 6.3 \pm 1$ ⁵⁶	55
18-crown-6	$\log K_d > 1$ ⁵⁷	35

Table 3: Standard Gibbs free energy of binding for Li^+ and Na^+ -crown ether complexes

Crown ether	$\Delta G_{\text{bind}}^\circ (\text{kJ mol}^{-1}), \text{Li}^+$	$\Delta G_{\text{bind}}^\circ (\text{kJ mol}^{-1}), \text{Na}^+$
12-crown-4	21.5141	19.8825
15-crown-5	19.1929	17.2118
18-crown-6	17.4659	21.7413